

Process design and economic evaluation for cyclopentane (CP)-based hydrate desalination

Parul Sahu

Salt and Marine Chemicals Division, CSIR – Central Salt and Marine Chemicals Research Institute, Bhavnagar, Gujarat – 364002, India, Tel. +91 278 2567760; email: paruls@csmcri.res.in

Received 10 August 2021; Accepted 6 January 2022

ABSTRACT

Clathrate hydrate desalination has emerged as an alternative to producing freshwater from seawater. There has been an increased interest towards the cyclopentane (CP) based hydrate desalination process in recent years. In this study, the process design and economic assessment have been carried out to establish the potential of CP-based hydrate desalination. Unlike previous studies reported to date, the present work considers detailed process design calculations and cost analysis using material and energy balance, equipment sizing, and economic estimations. Further, total capital investment estimates have been presented with profound specifics. The total capital investment for 1,000 m³/d desalinated water is estimated to be 7.19 million US\$ and the cost of water to be 5.71 \$/m³. The specific energy consumption for CP-based hydrate desalination is found to be 7.55 kWh/m³. Prospects of heat integration and waste energy utilization for improving the energy efficacy of CP hydrate desalination are also discussed. The techno-economic evaluation rationalizes the CP hydrate desalination technology worth considering for further development.

Keywords: Desalination; Cyclopentane; Hydrate desalination; Capital investment; Process design; Economic evaluation

1. Introduction

Clathrate hydrates are emerging as potential candidates for desalinating water from seawater/produced water/hypersaline water [1,2]. In the presence of a suitable hydrate forming agent (or hydrate former), in the gas phase (methane, ethane, propane, CO₂, etc.) or liquid phase (cyclopentane, refrigerants), host water molecules form cage-like structure entrapping the hydrate former. These structures (non-stoichiometric) are called hydrates and belong to compounds known as clathrates [3,4]. Interestingly, hydrates can be formed well above the freezing point of water under the suitable condition of temperature, pressure, and hydrate former. Apart from desalination, the clathrate hydrate process could be a promising method for recovering or purification of produced water (from oil/gas processing) and industrial wastewater [5].

It is well established that the selection of a suitable hydrate forming agent is crucial to the hydrate-based approach [6,7]. The hydrate desalination process using gaseous hydrate forming agents (i.e., propane, carbon dioxide, methane) requires high energy consumption during former recycling, increasing the overall energy requirement of the process [4,8]. Also, the required pressures for hydrate formation (4–40 times the atmospheric pressure) necessitate the hydrate crystallizer to operate at high pressure and increase the capital cost of the process [8]. More recently, cyclopentane (CP), a liquid-phase hydrate former, has drawn the attention of researchers as a potential hydrate forming agent owing to the following features:

- Using CP, hydrate formation pressure can be lowered to the atmospheric pressure with a relatively high formation temperature (above the freezing point of water) [8,9].

Therefore desalination by CP hydrate would be safer, and it would also reduce costs for the process to operate without pressurization [10].

- CP has low solubility in water (~0.156 g/L at 25°C) and is immiscible with water, allowing the easy separation of product water post-desalination [11,12].
- CP forms structure II hydrates (hydration number: 17), ensuring more water capture than structure I formers like methane, CO₂ [13].
- A moderate boiling point (~50°C) of CP makes it easy and safe to handle as a liquid [13].
- CP is readily available commercially and has a low cost [13].

Due to favorable hydrate formation conditions, CP hydrates are being explored for hydrogen storage and carbon dioxide capture application [14,15]. CP acts as a hydrate promoter for carbon capture and is used as a co-guest to milder hydrate formation conditions when combined with other molecules [7].

Recent studies focused on different aspects of salt removal from brine via the formation of CP hydrates [5,7,9,10,16–18]. Corak et al. [9] investigated the influence of subcooling and CP quantity on the rates of hydrate formation. Two subcooling temperatures of 5.6 and 3.6 K with respect to equilibrium temperature (6.6°C) for 3 wt.% NaCl solutions were investigated. Higher subcooling resulted in faster kinetics and a higher degree of desalination. However, the CP quantity was not significantly affect the hydrate formation rate and water purity. Han et al. [16] examined the successive secondary treatment of CP hydrates to improve salt removal efficiency. First, a CP hydrate formation reaction was carried out at 4.0°C (2.6 K super-cooling) and 3 mol% CP in a 3.5 wt.% NaCl solution. A few small ice particles were added to the crystallizer at the experimental temperature to commence hydrate formation quickly. After sufficient hydrate formation, the hydrate crystals were separated from the remaining liquid consisting of un-hydrate brine and CP. The filtered hydrates were subjected to centrifuging, washing, and sweating as secondary treatment. While centrifuging resulted in the best salt removal efficiency (~96%), the method could be energy-intensive and inefficient for large-scale applications. Washing with a small amount of wash water effectively removed the salt

adhered to hydrate crystals (~93%). Sweating for an appropriate amount of time reduced the salt attached to the crystal surface (~95%), but at the cost of a diminished amount of product water. The authors concluded that washing is a promising method to raise the efficiency of the CP hydrate-based desalination process.

Lv et al. [10] examined the CP hydrate kinetics in brine – CP dispersion systems in the context of desalination. An excess amount of CP (~12 mol%) into the brine – CP dispersion system increased the overall product water yield with 80% removal efficiency. The salt removal efficiency was enhanced with washing at a high ratio of washing water/dissociated water (~0.5). Xu et al. [17] investigated CP hydrate formation using a column crystallizer with two injection methods: tubing injection and spray injection. After hydrate formation, a three-step process including gravitational separation, filtration, and washing was adopted to improve the separation efficiency of hydrate-based desalination. The spray injection method resulted in more water conversion to hydrates because of the fine CP droplet sizes created by spray injection. Overall, 81% desalination efficiency was reported at optimized operating conditions and the three-step separation method.

Apart from lab-scale and pilot studies related to process advancement, the economic estimations of hydrate desalination have also been reported. Javanmardi and Moshfeghian [4] carried out the economic evaluation of the propane former-based hydrate desalination process in comparison to thermal (MSF, ME) and membrane (RO) processes. About hydrate desalination, they have reported the total work required for producing 1 m³ of potable water to be 25.82 and 172.38 MJ using propane and carbon dioxide as hydrate formers, respectively. A computer-aided program was used to estimate the energetics and costs of the hydrate desalination process without disclosing the details of the approach undertaken [4]. In a series of publications, a group of researchers from Singapore and China established the techno-economic feasibility of hydrate-based desalination utilizing cold energy from liquefied natural gas (LNG) [8,19,20]. However, commercial software (Aspen Hysys, Aspen ICARUS, and Aspen process economic analyzer) was used for process simulation, energy estimation, and costing. It is evident that there is still a need for economic analysis of the hydrate desalination system using a generic approach.

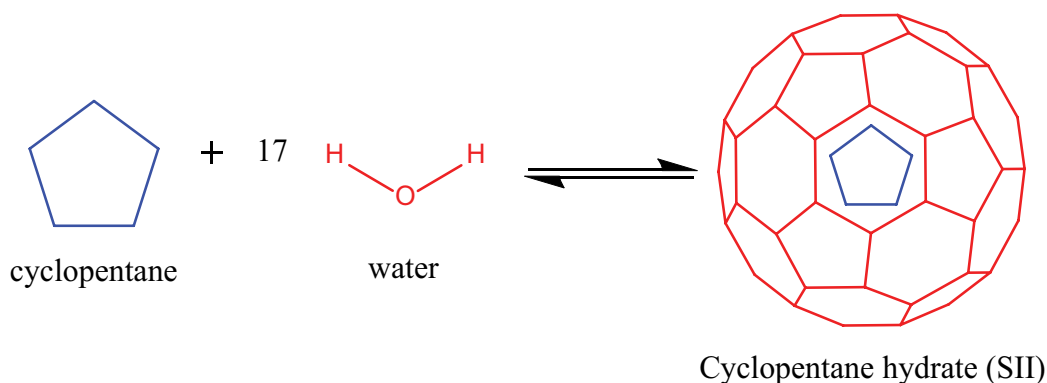


Fig. 1. Reaction representing CP hydrate formation.

This work aims to supplement the existing literature with regard to evaluating the techno-economic feasibility of cyclopentane (CP)-based hydrate desalination using process calculations and cost estimates.

2. Methodology

2.1. Process synthesis and calculations

2.1.1. Cyclopentane hydrate-based desalination process

CP has been selected as hydrate former for structure II (SII) hydrates in the present study. The following reaction represents the formation of cyclopentane (CP) hydrate formation:

Based on the previous studies on CP hydrate-based desalination discussed in section 1, the following notion has been considered for process calculations and analysis.

Starting with 3.5 wt.% salt (assuming pure NaCl for simplification) feed composition, the salt concentration is expected to increase with water removal during hydrate formation. Fig. 2a indicates the NaCl concentration in residual brine with water conversion (WC) during hydrate formation. This increase in brine concentration, in turn, will decrease the equilibrium hydrate formation temperature (T_{hyd}), as shown in Fig. 2b. For 50% seawater conversion to hydrate, the T_{hyd} will change from 5.6°C to 3°C. Therefore, the hydrate crystallizer temperature must be maintained at $\leq 3^\circ\text{C}$ to provide sufficient driving force for hydrate formation.

Fig. 3 presents a process flow sheet of CP hydrate-based desalination. This flowsheet is designed based on the work of Javanmardi and Moshfeghian [4] and Mottet [21].

The flowsheet comprises two pumps (P1 and P2), two heat exchangers (HE1 and HE2), a mixing tank with a homogenizer (MX), hydrate crystallizer (HC), vacuum filter (VF), wash column (W), melter (M), two decanters (D1 and D2), compressor (C) and expansion valve (EV).

As shown in Fig. 3, seawater (SW) is pressurized using pump P1 and sent to EX1. Seawater is pre-cooled in EX1 by exchanging heat with brine + cyclopentane (CP) stream. This pre-cooled seawater is mixed with wash water (WW) from the wash column (W), and the resultant stream is sent to the mixing tank with homogenizer (MX). The CP stream is also sent to MX, where it is mixed vigorously with SW before entering the hydrate crystallizer (HC). In HC, hydrate formation is facilitated by bringing the crystallizer temperature below the hydrate formation equilibrium temperature (6.6°C) and adding ice/hydrate seed to trigger the nucleation and growth. An external refrigeration cycle using R (HFC-134a) as a refrigerant is selected to maintain the formation temperature in HC. After sufficient hydrate crystals conversion (~50%), the hydrate slurry along with residual brine and unreacted CP is directed to a vacuum filter (VF). It is reported that the water molecules containing salt ions can be confined within the solid crystal of hydrate. Hence, a subsequent post-treatment is required to enhance salt removal efficiency. Optimized washing can be a promising method to raise the efficiency of the hydrate-based desalination process [5,16]. Thus, filtered hydrate crystals are transported to W for surface washing using a fraction of product water (~0.04). After washing, hydrate crystals are sent to a melter (M), where hydrate is dissociated into the liquid–liquid mixture of product water and CP. As CP

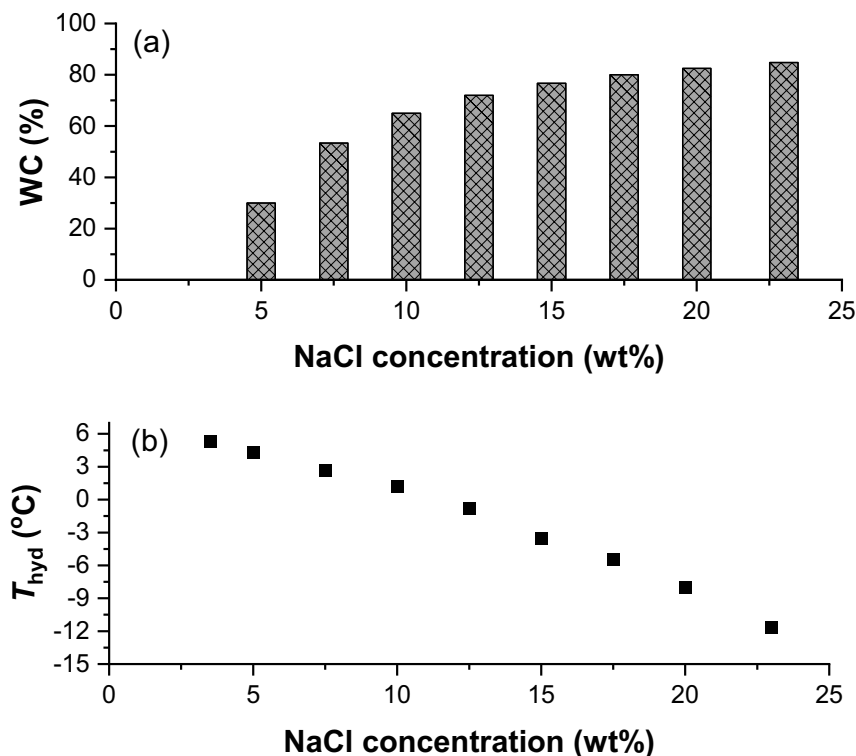


Fig. 2. (a) Percentage water conversion (WC) with NaCl concentration (b) CP hydrate formation temperature with NaCl concentration.

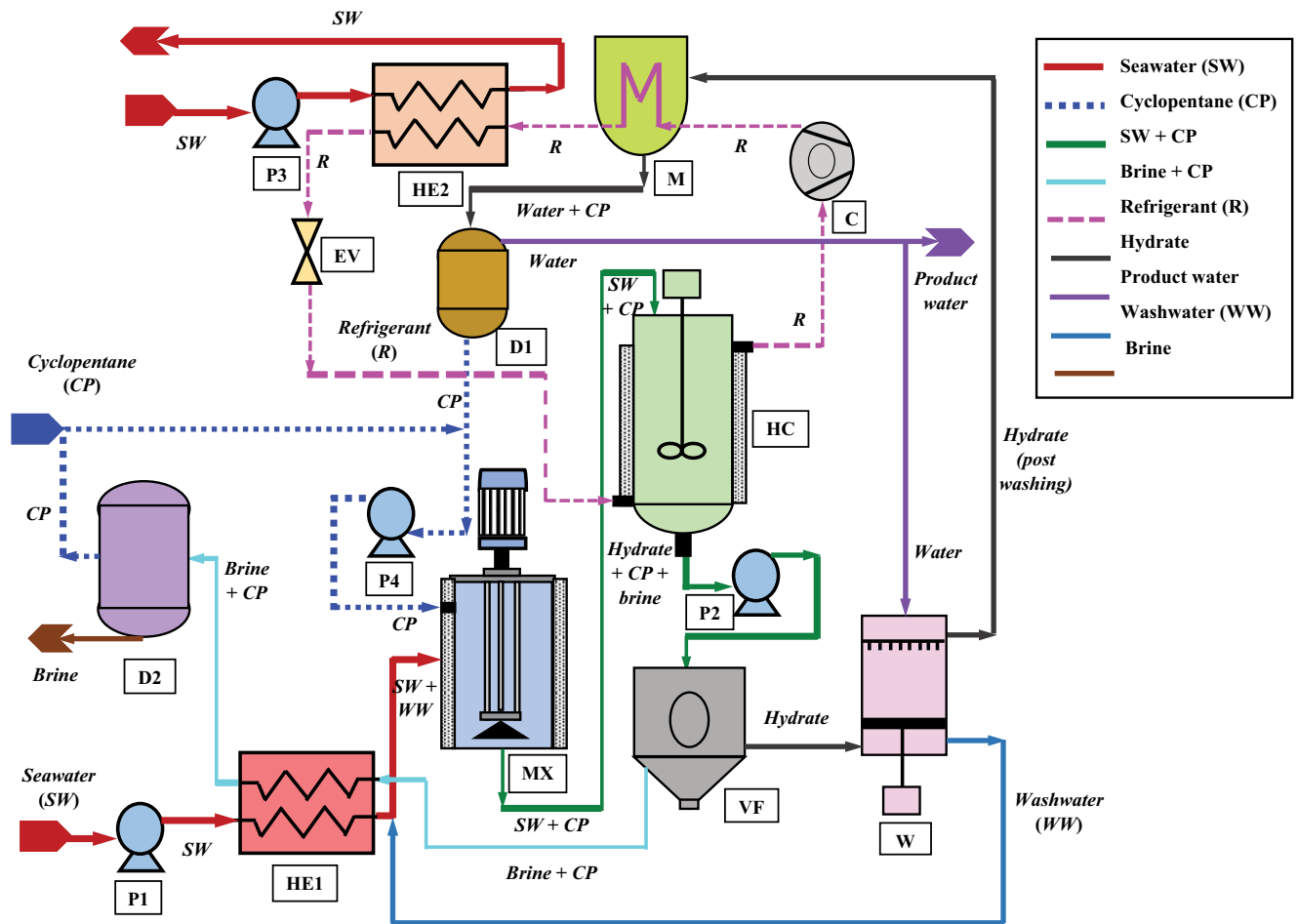


Fig. 3. Process flowsheet for cyclopentane hydrate desalination.

Table 1
Basis for process calculations and analysis

Basis	Value	References
Degree of super-cooling for hydrate formation	3.6 K	[5,9]
Cyclopentane mole% in seawater	3%	[5,16]
Conversion (feed seawater to hydrate)	50%	[5]
Hydrate melting temperature	282.15 K	[16]
Seawater composition	3.5 wt.% NaCl	[16]
Secondary treatment method	Washing	[16]
Wash water quantity (as % of the water obtained from hydrate)	4 wt.%	[16]

is nearly immiscible with water and shows extremely low mutual solubility [5], a decanter (D1) is used to separate CP from product water. CP is recycled back to MX for the next run.

The brine and CP mixture exiting the VF is sequentially sent to MX and EX1 to exchange the heat with inlet seawater. Subsequently, this mixed stream is sent to D2, where CP is separated from brine and recycled back to MX. A vapor-compression refrigeration system (discussed in section 2.1.4) is used to cool and promote hydrate formation in HC

and hydrate dissociation in M. While HC acts as an evaporator, M serves as a condenser for the refrigeration cycle. Additional seawater stream is employed for condensing the refrigerant in EX2 to continue the refrigeration loop.

2.1.2. Process conditions and assumptions

The process conditions and assumptions reported in Table 2 and thermo-physical properties presented in Table 3 were used to establish the material and energy balance.

Pressure drops and the heat losses to the environment from the HC, M, D1, D2, VF were neglected.

2.1.3. Material and energy balance

The heat exchanger, hydrate crystallizer, and melter heat duties are estimated using mass and energy balances for each unit of the hydrate production process shown in Fig. 3. Microsoft Excel spreadsheet tool was adopted for performing process calculations. The empirical equations and parameters were specified in the respective columns of the spreadsheet and outputs were generated.

For heat exchanger without phase change (EX1), the energy exchanged between two streams in the counter-current mode is estimated using Eq. (1) as shown below:

$$Q_{HE} = \dot{m}_h C_{p_h} (T_{h_o} - T_{h_i}) = \dot{m}_c C_{p_c} (T_{c_o} - T_{c_i}) \quad (1)$$

where \dot{m}_h and \dot{m}_c are the mass flow rates of the hot and cold streams, respectively, C_{p_h} and C_{p_c} are the specific heat capacities of the hot and cold streams, respectively, T_{h_o} and T_{h_i} are outlet and inlet temperature of hot stream respectively, T_{c_o} and T_{c_i} are outlet and inlet temperature of cold stream, respectively.

The heat transfer rate at the heat exchanger is expressed as:

$$Q_{HE} = UA\Delta T_{LMTD} \quad (2)$$

Table 2
Input process parameters/conditions

Assumption/process condition	Value
Seawater inlet temperature	300 K
Product water capacity	1,000 m ³ /d
Salt removal rate	100%
Total recovery of CP in a cycle	95%
Molar mass of CP hydrate	376.1 g/mol
Hydrate crystallizer temperature	276.15 K [5,9]
Melter temperature	288.15 K
Pressure drop across the heat exchanger	5 kPa
Minimum approaching temperature (ΔT_{min})	5 K
Adiabatic efficiency of pump and compressor	75%

Table 3
Thermo-physical properties

Property	Value	References
Density of seawater	1,025 kg/m ³	[22]
Density of CP hydrate	960 kg/m ³	[7]
Density of cyclopentane	751 kg/m ³	[7]
Specific heat capacity of seawater, $C_{p_{sw}}$	$2.407 + 1.496 \times 10^{-2} T - 4.776 \times 10^{-5} T^2 - 5.208 \times 10^{-8} T^3$ kJ/(k mol K)	[22]
Specific heat capacity of CP hydrate, $C_{p_{hyd}}$	$-124.33 + 3.2593T + 2 \times 10^{-6} T^2 - 4 \times 10^{-9} T^3$ kJ/(kg K)	[8]
Specific heat capacity of cyclopentane, $C_{p_{cp}}$	1.8 at 25°C (kJ/kg K)	[23]
Specific enthalpy of CP hydrate formation/dissociation	377 ± 27 kJ/kg of water	[24]

where U is the overall heat transfer coefficient, A is heat transfer area and ΔT_{LMTD} is a logarithmic mean temperature difference, estimated as:

$$\Delta T_{LMTD} = \frac{(T_{h_i} - T_{c_o}) - (T_{h_o} - T_{c_i})}{\ln \frac{(T_{h_i} - T_{c_o})}{(T_{h_o} - T_{c_i})}} \quad (3)$$

The total cooling load required for the hydrate crystallizer is the sum of sensible duty ($Q_{sensible,SW+CP}$) for precooling of seawater + CP mixture and latent duty ($Q_{latent,Hyd}$) of hydrate formation as:

$$Q_{sensible,SW+CP} = \dot{m}_{sw} C_{p_{sw}} (T_{HC} - T_i) + \dot{m}_{cp} C_{p_{cp}} (T_{HC} - T_i) \quad (4)$$

$$Q_{latent,Hyd} = \dot{m}_{Hyd} h_{Hyd\ formation} \quad (5)$$

where \dot{m}_{sw} and \dot{m}_{cp} are the mass flow rate of seawater and cyclopentane, respectively, kg/h; $C_{p_{sw}}$ and $C_{p_{cp}}$ are the specific heat capacity of seawater and cyclopentane, respectively, kJ/(kg K); T_{HC} and T_i are the hydrate crystallizer temperature and inlet temperature, respectively, K; \dot{m}_{Hyd} is the mass flow rate of hydrate, kg/h; $h_{Hyd\ formation}$ is the specific enthalpy of CP hydrate formation, kJ/kg of water.

The total heating load required for the melter is calculated as the sum of sensible duty ($Q_{sensible,Hyd}$) for hydrate heating to equilibrium hydrate dissociation temperature (279.75 K), latent duty ($Q_{latent,Hyd}$) of hydrate dissociation, and sensible duty ($Q_{sensible,SW+CP}$) for heating of dissociated seawater + CP mixture to melter temperature (288.15 K):

$$Q_{sensible,Hyd} = \dot{m}_{hyd} C_{p_{hyd}} (T_{hyd\ dissociation} - T_{HC}) \quad (6)$$

$$Q_{latent,HC} = \dot{m}_{hyd} h_{hyd\ dissociation} \quad (7)$$

$$Q_{sensible,SW+CP} = \dot{m}_{sw} C_{p_{sw}} (T_M - T_{hyd\ dissociation}) + \dot{m}_{cp} C_{p_{cp}} (T_M - T_{hyd\ dissociation}) \quad (8)$$

where $C_{p_{hyd}}$ is the specific heat capacity of cyclopentane hydrate, kJ/(kg·K); T_M and $T_{hydrate\ dissociation}$ are the melter temperature and equilibrium hydrate dissociation temperature, respectively, K; $h_{hyd\ dissociation}$ is the specific enthalpy of CP hydrate dissociation, kJ/kg of water.

2.1.4. Vapor compression refrigeration system

The layout of a vapor compression refrigeration system (VCRS) and the pressure–enthalpy ($P-H$) diagram are shown in Figs. 4a and b, respectively. An ideal refrigeration cycle, with R-134a as a refrigerant (R), comprised of isobaric evaporation (2→3), isentropic compression (3→4), isobaric condensation (4→1), and isenthalpic expansion (1→2) is considered. As shown in Fig. 4b, the refrigerant enters the evaporator as a two-phase mixture (liquid and vapor) at state 2, absorbs heat (Q_{ev}), and turns into saturated vapor (state 3). Subsequently, this saturated vapor is isentropically compressed to superheated vapor using a compressor to a higher temperature (T_{cond}) and pressure (P_{cond}). The refrigerant fluid enters the condenser as superheated vapor, undergoes a complete change to phase (condenses) in two distinct sections (M and HE2). Finally, the refrigerant undergoes an isenthalpic process through the expansion valve, entering as subcooled liquid (state 1) and exiting as a liquid–vapor mixture (state 2). The data reduction of the theoretical approach is presented below [25].

Isentropic compression work of the compressor (W_{comp}) is expressed as follows:

$$W_{comp} = \dot{m}_R (h_4 - h_3) \quad (9)$$

The heat transfer rate of the evaporator (Q_{ev}) is calculated as follows:

$$Q_{ev} = \dot{m}_R (h_3 - h_2) \quad (10)$$

where \dot{m}_R is refrigerant mass flow rate, h_i is the specific enthalpy of the refrigerant at i th (1 to 4) state (reported in Table 4).

The coefficient of performance (COP) of the refrigeration system's cycle can be estimated as:

$$COP = \frac{Q_{ev}}{W_{comp}} \quad (11)$$

The VCRS is integrated with the hydrate formation and dissociation process (presented in Fig. 3). In this integrated refrigeration cycle, the total cooling load of HC is provided by the latent heat of evaporation of the refrigerant, thus:

$$Q_{ev} = Q_{sensible, SW+CP} + Q_{latent, Hyd} \quad (12)$$

Refrigerant mass flow rate (\dot{m}_R) is estimated using Eqs. (10) and (12). Subsequently, the heat transfer rate to the condenser (Q_{cond}) is calculated as:

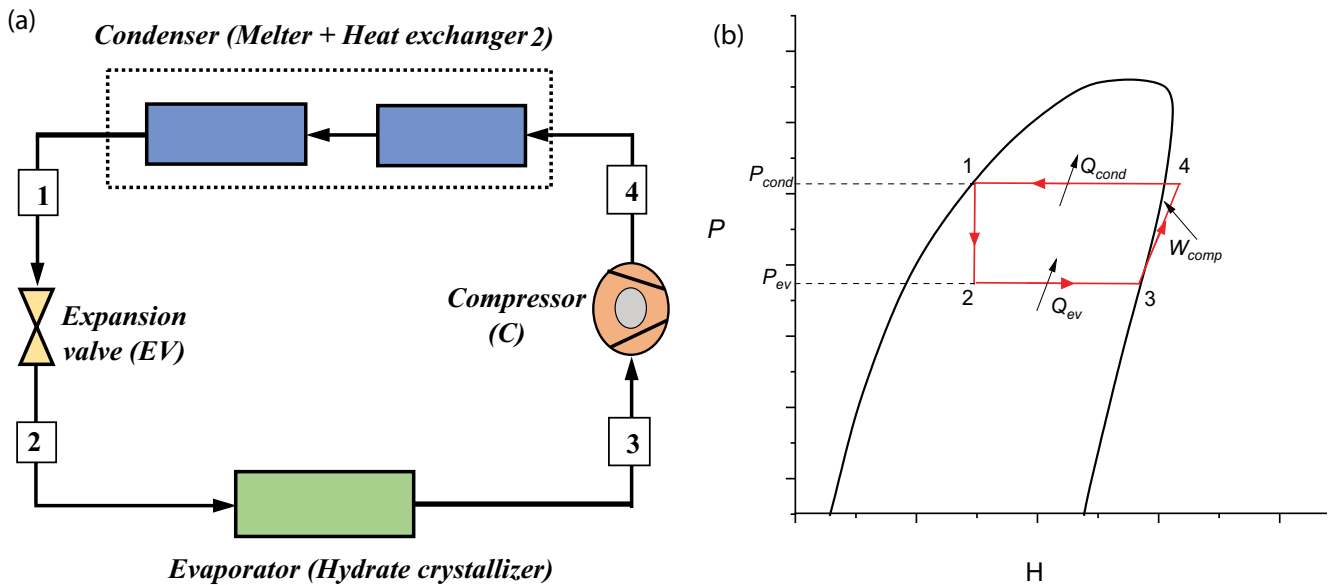


Fig. 4. (a) Layout of the vapor compression refrigeration system used in the hydrate desalination process and (b) vapor compression refrigeration cycle on $P-H$ diagram.

Table 4
Thermodynamic properties of R134a

State	Temperature, T (K)	Pressure, P (bar)	Specific enthalpy, h (kJ/kg)
1 (Saturated liquid)	291.15	6	230
2 (Two-phase mixture)	273.15	3	230
3 (Saturated vapor)	273.15	3	400
4 (Superheated vapor)	291.15	6	415

$$Q_{\text{cond}} = \dot{m}_R (h_1 - h_4) \quad (13)$$

A minimum approach temperature of 3 K is considered across the hydrate crystallizer and melter. The refrigerant temperature in the evaporator (T_{ev}) and condenser (T_{cond}) is deduced to be 273.15 and 291.15 K, respectively. Thermodynamic states (T and P) and specific enthalpy (h) of the refrigerant at different points of the refrigeration cycle are obtained from the literature [26] and reported in Table 4.

2.2. Economic evaluation

After process design, complete material and energy balance, equipment sizing, and selection of materials of construction, a preliminary estimate method (based on the individual factors method of Guthrie) has been used for cost estimations employing Microsoft Excel spreadsheet program. Unified units (SI system) was adopted and appropriate unit conversion from fps system to SI system were considered.

2.2.1. Total capital investment

The total capital investment (C_{TCl}) of a plant includes the expenses to supply the necessary manufacturing and plant facilities and operations [27]. According to the Guthrie method [28], the total capital investment can be estimated as:

$$C_{\text{TCl}} = C_{\text{TPI}} + C_{\text{WC}} = 1.18 \left(C_{\text{TBM}} + C_{\text{site}} + C_{\text{buildings}} + C_{\text{off-site facilities}} \right) + C_{\text{WC}} \quad (14)$$

where, C_{TPI} is the total permanent investment (or fixed capital investment), a one-time expense for the design, erection, and start-up of a new plant. C_{WC} is working capital that covers operating costs required for the early operation of the plant, including the cost of the inventory and funds to cover accounts receivable. The factor 1.18 in Eq. (16) accounts for a contingency of 15% and a contractor fee of 3%. Details of other cost components of Eq. (14) are discussed in the following section.

2.2.1.1. Total bare-module cost

Total bare-module cost (C_{TBM}) is the capital necessary for installing process equipments with all components needed for complete process operation. Firstly, the free on board (f.o.b.) purchase cost of each piece of major equipment (for the process shown in Fig. 3) has been estimated at the base cost index, I_B (The Chemical Engineering (CE) plant cost index, the year 2000) [28]. Table 5 shows the equations used to calculate the purchase costs (f.o.b.), C_p in US\$, of significant equipments and machineries. Stainless steel (SS 316) is considered as material of construction (MOC), and accordingly, a material factor (F_M) is used wherever applicable.

After estimating the purchase costs of equipment, the direct costs of materials and labor and indirect costs involved in the installation procedure need to be taken into account. The total installed costs are called the bare-module

costs (C_{BM}) and a bare-module factor F_{BM} is given for each equipment by Guthrie (Table 6).

The bare-module cost of equipment can be calculated using:

$$C_{\text{BM}} = F_{\text{BM}} C_p \left(\frac{I}{I_B} \right) \quad (15)$$

where F_{BM} = bare-module factor; C_p = f.o.b. purchase cost; I_B = base cost index (394); I = latest cost index (600).

The chemical engineering (CE) plant cost index $I = 600$ for year 2019 is used for updating the cost correlations [29]. Bare-module factors of Guthrie (1974) for ordinary materials of construction and low-to-moderate pressures were considered for the estimation of C_{BM} are presented in Table 6.

Total bare-module cost (C_{TBM}) is estimated by summing the bare module cost (C_{BM}) of different types of equipment, as given in Eq. (16):

$$C_{\text{TBM}} = \sum C_{\text{BM}} \quad (16)$$

2.2.1.2. Other costs

Other indirect costs for plant components not directly related to the process operation (i.e., land, processing buildings, warehouse, laboratories, and other permanent parts of the plants) are approximated as a fraction of C_{TBM} . C_{site} is site development costs (10%–20% of C_{TBM} may be assigned). $C_{\text{buildings}}$ is building costs that include process buildings and non-process buildings. If the equipment is housed, the cost of process buildings may be estimated at 10% of C_{TBM} . For a grass-root plant, the non-process buildings may be assessed at 20% of C_{TBM} . $C_{\text{offsite facilities}}$ involve the costs of off-site facilities, including utility, pollution control, waste treatment, off-site tankage, and receiving and shipping facilities, etc. It is estimated as 10% of C_{TBM} .

2.2.1.3. Working capital

Working capital includes the continuing costs associated with the operation of the plant. The desalination plant requires inexpensive feedstock, that is, seawater (a natural resource). Major components of C_{WC} are expenses on utility $C_{\text{Utilities}}$, operation and maintenance $C_{\text{O\&M}}$, taxes and insurance $C_{\text{T\&I}}$ and depreciation $C_{\text{Depreciation}}$ [28].

$$C_{\text{WC}} = C_{\text{Utilities}} + C_{\text{O\&M}} + C_{\text{T\&I}} + C_{\text{Depreciation}} \quad (17)$$

Electricity is the primary utility for the hydrate desalination plant. The approximate power consumption of pumps, compressors, agitator motors, and vacuum units is 9420 kWh/d. It is assumed that the electricity cost is \$0.07/kWh.

Plant operating cost primarily comprises direct wages and benefits (DW&B), calculated from an hourly rate for the operators of the proposed plant. For preliminary estimates of the number of operators required per shift, the process is divided into sections, that is, (1) feed preparation, (2) hydrate crystallization system, (3) refrigeration

Table 5
Equations used to calculate the purchase cost (f.o.b.), C_p , of equipments and machinery, indexed to mid-2000 ($I_B = 394$) [28]

Equipment	Equations used for f.o.b. calculation	Nomenclature
Pump	$S = Q(H)^{0.5}$	S = size factor
	$C_B = \exp[9.2951 - 0.6019(\ln S) + 0.0519(\ln S)^2]$	Q = flow rate in gallons per minute H = pump head in feet
	$C_p = F_M C_B$	C_B = base costs F_M = material factor (2 for SS)
	$P_C = \frac{P_T}{\eta_p \eta_M} = \frac{P_B}{\eta_M} = \frac{QH_p}{33,000 \eta_p \eta_M}$	P_C = power consumption P_T = theoretical horsepower of the pump η_p = fractional efficiency of the pump η_M = fractional efficiency of the electric motor
	$\eta_p = -0.316 + 0.24015(\ln Q) - 0.01199(\ln Q)^2$	Q = flow rate through the pump in gallons per minute
	$\eta_M = 0.80 + 0.0319(\ln P_B) - 0.00182(\ln P_B)^2$	H = pump head in feet of fluid flowing P_B = pump brake horsepower
	$C_B = \exp[5.4866 + 0.13141(\ln P_C) + 0.053255(\ln P_C)^2 + 0.028628(\ln P_C)^3 - 0.0035549(\ln P_C)^4]$	ρ = liquid density in pounds per gallon C_B = base costs
	$C_p = F_T C_B$	F_T = motor-type factor (1.4 for totally enclosed, fan-cooled)
	$C_B = \exp[11.0545 - 0.92228(\ln A) + 0.09861(\ln A)^2]$	A = heat exchange area in ft ² C_B = base costs
	$F_M = 2.70 + \left(\frac{A}{100}\right)^{0.07}$	F_p = pressure factor (1.01 based on shell-side pressure) F_M = material factor for SS shell and tube F_L = tube-length correction (1.25 for tube-length of 8 ft)
Heat exchanger and melter		
Hydrate crystallizer	$C_p = F_p F_M F_L C_B$	L = length (ft) C_B = base costs F_M = material factor (2 for SS)
	$C_B = 11,400 L^{0.67}$	
	$C_p = F_M C_B$	

(Continued)

Table 5 Continued

Equipment	Equations used for f.o.b. calculation	Nomenclature
Compressor	$P_B = 0.00436 \left(\frac{k}{k-1} \right) \frac{Q_i P_i}{\eta_B} \left[\left(\frac{P_O}{P_i} \right)^{\frac{k-1}{k}} - 1 \right]$ $\eta_M = 0.80 + 0.0319 (\ln P_B) - 0.00182 (\ln P_B)^2$ $P_C = \frac{P_B}{\eta_M}$ $C_B = \exp[7.2223 + 0.80 (\ln P_C)]$	<p>P_B = brake horsepower Q_i = inlet volumetric flow rate in cubic feet per minute P_i = pressure at the inlet in lbf/in² P_O = pressure at the outlet in lbf/in² k = constant specific heat ratio (1.15 for HFC-134a) η_B = isentropic efficiency of the electric motor η_M = fractional efficiency of the electric motor P_C = power consumption C_B = base costs F_D = drive factor (1 for motor drive) F_M = material factor (2 for SS)</p>
Decanter	$C_P = F_D F_M C_B$ $S = H(D)^{0.5}$ $C_B = 250(S)^{0.84}$ $C_P = F_M C_B$ $C_B = 210(V)^{0.51}$ $C_P = F_M C_B$ $C_B = 2600(S)^{0.17}$ $C_P = F_M C_B$ $C_B = 960(A)^{0.52}$ $C_P = F_M C_B$	<p>S = size factor H = Height in feet D = Height in feet C_B = base costs F_M = material factor (2.5 for SS) V = Vessel volume in gallon C_B = base costs F_M = material factor (2.5 for SS) S = motor horsepower (1.5 hp for 1000 gallon) C_B = base costs F_M = material factor (2.5 for SS) A = filtering area in ft² C_B = base costs F_M = material factor (2 for SS)</p>
Mixing tank	$W = \pi (D_i + t_s)(L + 0.8D_i)t_s \rho$ $C_V = \exp[7.0374 + 0.18255 (\ln W) + 0.02296 (\ln W)^2]$ $C_{PL} = 237.1(D_i)^{0.63316} (L)^{0.80161}$ $C_P = F_M C_V + C_{PL}$	<p>W = weight of the column in lb L = column length in feet D_i = inside diameter in feet t_s = wall thickness (3/8 inch) ρ = density of material of construction (0.29 lb/inch³ for SS) C_V = vertical column cost C_{PL} = cost for platforms and ladders F_M = material factor (2 for SS)</p>
Agitator (for mixing tank)		
Vacuum filter		
Wash column		

Table 6
Bare-module factors of Guthrie (1974) [28]

Equipment	Bare-module factor (F_{BM})
Shell and tube heat exchanger, Melter	3.17
Pumps	3.3
Crystallizers	2.06
Compressors	2.15
Filters	2.32
Other equipment	2.6*

*Arithmetic mean of F_{BM} is considered for other equipments.

system, (4) CP recovery system, (5) slurry-hydrate separation system, and (6) residual liquid abatement system. For a continuously operating, automatically controlled plant, two operators/shift can be assigned per shift. Each shift operator is paid for 40 h/wk and 52 wk/y. Commonly five shifts for each operator are required. The annual cost of DW&B is obtained from [28]:

$$DW \& B, \$/y = \left(\frac{\text{Operators}}{\text{shift}} \times 5 \text{ shifts} \times 2,080 \frac{\text{hr}}{\text{year} - \text{operator}} \times \frac{\$}{\text{h}} \right) \quad (18)$$

The cost for maintenance of a proposed plant is also an essential component of C_{WC} and can be assumed 10% of C_{TPI} . $C_{T\&I}$ and $C_{\text{Depreciation}}$ costs are approximated to 2% and 8% of C_{TPI} , respectively [28].

2.2.2. Amortized total investment and product cost

Amortized total investment, including the capital, operation, and maintenance (O&M) costs, were estimated using the method adopted by Javanmardi and Moshfeghian [4]; Javanmardi et al. [30]. Assuming 20 y of plant life and 8% of a continuous discount rate, the amortized capital investment is obtained using the following equation.

$$C_{ACI} = \frac{\left(\frac{e^{(0.08 \times 20)}}{\sum_{i=0}^{19} e^{(0.08 \times i)}} \times C_{TPI} \right)}{(365 \times \text{Capacity})} \quad (19)$$

Amortized operation and maintenance (O&M) costs were obtained using.

$$C_{AO\&M} = \frac{C_{WC}}{\text{Capacity}} \quad (20)$$

Finally, the total product cost is estimated as the sum of the amortized capital investment and O&M costs.

$$\text{Total product cost} = C_{ACI} + C_{AO\&M} \quad (21)$$

Table 7
Specifications of different equipments of the CP hydrate desalination process, obtained from mass and energy balances

Equipment	Heat duty/Power
Heat exchanger (HE 1)	Duty: 832 kW
Heat exchanger (HE 2)	Duty: 409 kW
Pump (P1)	Power: 4.50 kW
Pump (P2)	Power: 6.33 kW
Pump (P3)	Power: 2.00 kW
Pump (P4)	Power: 0.50 kW

3. Results and discussion

The output generated from Microsoft Excel spreadsheet program for material and energy balance and plant economic are presented.

3.1. Material and energy balance

Considering 50% of seawater conversion to hydrate (and thereafter product water), a seawater feed flow rate, m_{sw} of 2,000 ton/d is required for generating 1,000 ton/d (or 1,000 m³/d) of product water m_{pw} . The output, including heat exchanger duty, and pump power, are presented in Table 7. The overall heat transfer coefficient, U equal to 1,200 W/(m² K), is used for estimating the heat exchanger area of HE 1 and HE 2.

The heat load of the hydrate crystallizer estimated using Eqs. (4) and (5) is 138.42 kWh/m³ of water. Assuming heat gain from ambient to the cooling system is 5% of total load, the total cooling load will be 145.34 kWh/m³. The enthalpy of hydrate dissociation should be provided in the melter. Thus, it acts as a heat exchanger, and a double-pipe model is used for design.

Vapor compression refrigeration system operating parameters at $T_{\text{ev}} = 273.15$ K and $T_{\text{cond}} = 291.15$ K are presented in Table 8.

3.2. Plant economics

The equipment list is prepared to incorporate the equipment title, label, size, and specifications for the CP hydrate desalination process. Subsequently, the purchase f.o.b. costs at a CE index of 390 are estimated using the equations tabulated in Table 5. Stainless steel (SS 316) has been considered as the material of construction (MOC) for all the equipments and machinery. Purchase f.o.b. costs were factored by F_{BM} and updated for the latest index (I) for the year 2019 to obtain the bare-module cost of equipment. Table 9 shows the equipment list with size/specifications and bare-module cost (C_{BM}). Accordingly, the total bare-module cost (C_{TBM}) for the CP-hydrate desalination process is 3.92 million US\$ (M\$). The percentage breakdown of C_{TBM} is presented in Fig. 5. The primary equipments contributing to installed equipment costs are compressor, hydrate – crystallizer, and decanters.

The onsite costs correspond to the bare-module equipment costs for the items shown in Fig. 3 were estimated directly from Guthrie's correlations. Various cost components

described in section 2.2.1.2 were calculated. The results are reported in Table 10.

The percent breakdown of total permanent investment (C_{TPI}) is also summarized in Fig. 6. It can be seen that the bare-module equipment costs account for around 69% of the total permanent investment.

A summary of cost estimates performed in this work is summarized and compared with the data reported in the literature as shown in Table 11. The cost-estimations reported by Chong et al. [20] and He et al. [8] are expected to be much less than the projected costs in this work, as the cold-energy source (LNG) helps to eliminate the entire refrigeration cycle and to reduce the overall process costs. For the given product water capacity of 1,000 m³/d, the specific energy consumption in the present work is

slightly higher than the value reported by Javanmardi and Moshfeghian [4]. This may be because the process they described uses two pumps, whereas the present process incorporates four pumps in total. The current process's total capital investment and total product costs are also on the higher side. This might be due to an increase in the cost index between 2002 and 2019 (17 y). The estimated

Table 8
Operating parameters of VCRS

Parameter	Value
Refrigerant	R134a (1,1,1,2-tetrafluoroethane)
\dot{m}_R	3,049 ton/d
P_{ev}	3 bar
P_{cond}	6 bar
W_{comp}	530 kW
COP	11.33

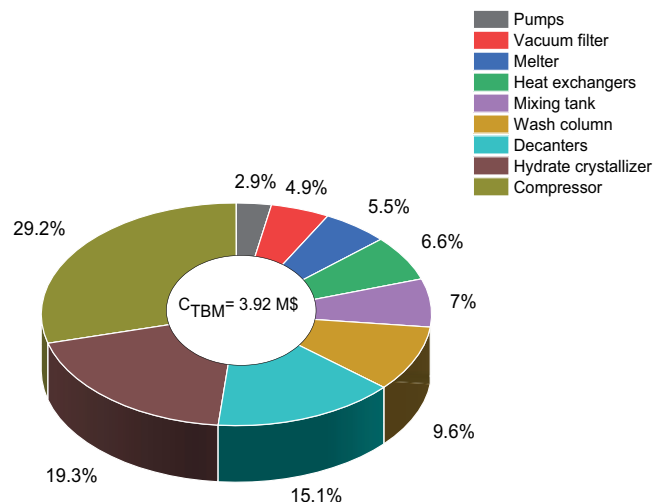


Fig. 5. Breakdown of total bare-module costs for CP-hydrate desalination process.

Table 9
Equipment list with sizing and bare-module costs (C_{BM}) at $I = 600$

Equipment title and label	Size/specifications	Bare-module costs (C_{BM}) in US\$
Seawater pump: P1 (including electric motor)	Seawater flow rate = 81 m ³ /h Motor brake power = 8 hp	27,091.5
Hydrate slurry pump: P2	Slurry flow rate = 95.4 m ³ /h Motor brake power = 25.5 hp	23,744.8
Seawater pump: P3	Seawater flow rate = 60 m ³ /h Motor brake power = 3.8 hp	20,879.7
Cyclopentane pump: P4	Cyclopentane flow rate = 14 m ³ /h Motor brake power = 1.4 hp	134,028.1
Heat exchanger (Seawater –brine): HE1	Heat exchange area = 77 m ²	124,447.2
Heat exchanger (Seawater – refrigerant): HE2	Heat exchange area = 63 m ²	274,431.4
Mixing tank with homogenizer: MX	Volume = 48.3 m ³ Mixing time = 30 min	757,521.8
Hydrate crystallizer: HC	Volume = 106.5 m ³ Residence time = 60 min	41,323.8
Vacuum filter: VF	Filter area = 27.2 m ²	191,127.8
Wash column: W	Volume = 20.3 m ³ Washing time = 20 min	374,922.4
Melter: M	Heat exchange area = 204 m ²	215,906.6
Decanter (CP – brine): D1	Volume = 27 m ³ Holdup time = 24 min	341,784.1
Decanter (CP – product water): D2	Volume = 17 m ³ Holdup time = 20 min	1,145,611
Compressor: C	Brake power = 424 hp	250,825.6

total product cost of water from CP hydrate desalination is 5.71 \$/m³, which is higher than the commercial reverse osmosis desalination (~3 \$/m³ for 1,000 m³/d capacity [31]).

4. Scope for heat integration/waste energy utilization

The process economics presented in the previous section uses a basic process sequence approach. It requires optimization utilizing a heat exchanger network (HEN) to further cut energy and operating costs. The application of advanced refrigeration cycles offering a high coefficient of performance (COP) can enhance the energy efficiency of the external refrigeration cycle, contributing to major energy costs in the entire hydrate desalination process.

Utilization of the potential refrigeration available in low-temperature liquefied natural gas (LNG) during regasification in an integrated manner has already been well established by researchers [8,19,20,32,33]. The enthalpy

of the cold LNG stream is used to cool the hydrate former and seawater to the hydrate formation temperature in the crystallizer, which can significantly reduce the energy consumption of the desalination process by replacing the refrigeration cycle. Depending upon the hydrate forming agent applied for hydrate desalination, the overall energy consumption is reported to be reduced to 0.84 kWh/m³ (for propane) [20] and 0.35 kWh/m³ (for CP) [8]. This hybrid concept can potentially be extended in practice to reduce the energy requirement for the external refrigeration cycles used in the present study. Nonetheless, such an integration would need a stable LNG cold energy source.

5. Conclusions

This work develops and presents the Microsoft Excel spreadsheet program-based process calculations and economic estimations for the cyclopentane-based hydrate desalination. The process calculations reported in this work can be used as fundamental design values to synthesize the CP hydrate-based desalination process. The total capital investment is 7.19 M\$ for 1,000 m³/d freshwater production

Table 10
Cost components for 1,000 ton/d (~1,000 m³/d) product water from CP hydrate desalination

Cost component	Value in US\$
Total bare-module costs (C_{TBM}): I	3,923,646
Site development costs (C_{site}): II	392,365
Building costs ($C_{buildings}$): III	980,912
Off-site facilities costs ($C_{offsite\ facilities}$): IV	392,365
Total permanent investment (C_{TPI}): (I + II + III + IV) = V	5,689,288
	Value in US\$/y
Utility ($C_{Utilities}$): VI	184,803
*Direct wages and benefits (DW&B): VII	1,248,000
Operating cost: VIII	28,447
Tax and insurance ($C_{T\&I}$): IX	5,689
Depreciation ($C_{Depreciation}$): X	22,757
Working capital (C_{WC}): (VI + VII + VIII + IX + X) = XI	1,489,696

*\$15/h wages and benefits are considered.

Table 11
Comparison of CP hydrate desalination process with other hydrate former based desalination processes

Parameters	Javanmardi and Moshfeghian [4]	Chong et al. [20]	He et al. [8]	Present work
Cost index year	2002	2017	Not reported	2019
Hydrate former	Propane	Propane	Cyclopentane	Cyclopentane
Product water capacity, m ³ /d	1,000	6,200	1,800	1,000
Specific energy consumption*, MJ/m ³	25.82	3.02 (with cold energy integration)	1.26 (with cold energy integration)	27
Total capital investment, M\$	5.46	9.6	6.11	7.19
Total product cost, \$/m ³	2.76	1.11 (with cold energy integration)	Not reported	5.71 \$/m ³

*Specific energy consumption estimated as total work of compressor and pump.

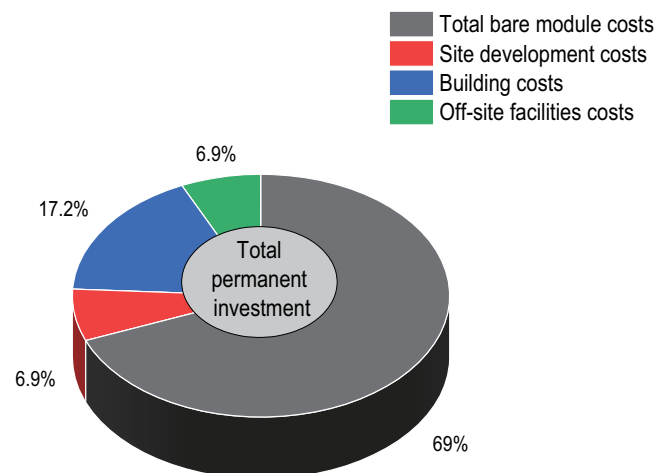


Fig. 6. Breakdown of total permanent investment (fixed capital investment) for CP-hydrate desalination process.

using the CP hydrate desalination process. The cost estimates rationalize the CP hydrate desalination technology worth considering for further development. The specific energy consumption for the proposed hydrate desalination process is estimated to be 7.55 kWh/m³ product water, which is considerably higher than the existing desalination technologies (i.e., reverse osmosis). However, the reverse osmosis process faces challenges of membrane fouling and disposal of membrane waste. Hydrate desalination technology can be an alternate, and further optimization using heat integration and/or cold energy integration can decrease the capital and operating costs to make the CP hydrate desalination process attractive. The prospect of hybrid hydrate and membrane processes to improve the overall desalination efficiency with maximum energy recovery and to treat hyper-saline water are other areas with increasing interest and research [2,34].

Symbols

A	—	Heat transfer area, m ²
C_{ACI}	—	Amortized capital investment
$C_{AO\&M}$	—	Amortized operation and maintenance costs
C_{BM}	—	Bare-module cost of equipment, US\$
$C_{buildings}$	—	Building costs, US\$
$C_{Depreciation}$	—	Depreciation costs, US\$
$C_{O\&M}$	—	Operation and maintenance costs, US\$/y
$C_{off-site facilities}$	—	Costs of off-site facilities, US\$
C_P	—	free on board (f.o.b.) purchase cost of equipment
C_{P_c}	—	Specific heat capacity of the cold stream, kJ/(kg K)
$C_{P_{CP}}$	—	Specific heat capacity of cyclopentane, kJ/(kg K)
C_{P_h}	—	Specific heat capacity of the hot stream, kJ/(kg K)
$C_{P_{hyd}}$	—	Specific heat capacity of cyclopentane hydrate, kJ/(kg K)
$C_{P_{SW}}$	—	Specific heat capacity of seawater, kJ/(kg K)
C_{site}	—	Site development costs, US\$
$C_{T\&I}$	—	Taxes and insurance costs
C_{TBM}	—	Total bare-module cost, US\$
C_{TCI}	—	Total capital investment
C_{TPI}	—	Total permanent investment, US\$
$C_{Utilities}$	—	Costs for utilities, US\$/y
C_{WC}	—	Working capital, US\$/y
CO_2	—	Carbon dioxide
COP	—	Coefficient of performance
CP	—	Cyclopentane
$DW\&B$	—	Direct wages and benefits, US\$/y
F_{BM}	—	Bare-module factor
F_M	—	Material factor
$h_{hyd formation}$	—	Specific enthalpy of cyclopentane hydrate formation, kJ/kg of water
$h_{hyd dissociation}$	—	Specific enthalpy of cyclopentane hydrate dissociation, kJ/kg of water
h_i	—	Specific enthalpy of refrigerant at <i>i</i> th state, kJ/kg
I	—	Latest cost index

I_B	—	Base cost index
ME	—	Multi-effect evaporation
MSF	—	Multi stage flash
MOC	—	Materials of construction
\dot{m}_c	—	Mass flow rate of the cold stream
\dot{m}_{CP}	—	Mass flow rate of cyclopentane
\dot{m}_h	—	Mass flow rate of the hot stream
\dot{m}_R	—	Mass flow rate of refrigerant, ton/d
\dot{m}_{SW}	—	Mass flow rate of seawater
P_{cond}	—	Condenser operating pressure, bar
P_{ev}	—	Evaporator operating pressure, bar
Q_{cond}	—	Heat transfer rate to the condenser
Q_{ev}	—	Heat transfer rate to the evaporator
Q_{HE}	—	Heat exchanger duty, kW
Q_{latent}	—	Latent heat duty
$Q_{sensible}$	—	Sensible heat duty
RO	—	Reverse osmosis
SII	—	Structure II
T_{c_i}	—	Inlet temperature of the cold stream, K
T_{c_o}	—	Outlet temperature of the cold stream, K
T_{HC}	—	Hydrate crystallizer bulk temperature, K
T_{h_i}	—	Inlet temperature of the hot stream, K
T_{h_o}	—	Outlet temperature of the hot stream, K
$T_{hyd dissociation}$	—	Equilibrium hydrate dissociation temperature, K
T_i	—	Inlet temperature, K
T_M	—	Melter temperature, K
ΔT_{LMTD}	—	Log mean temperature difference (K)
U	—	Overall heat transfer coefficient, W/(m ² K)
W_{comp}	—	Isentropic compression work of the compressor, kW

References

- [1] N. Gaikwad, R. Nakka, V. Khavala, A. Bhadani, H. Mamane, R. Kumar, Gas hydrate-based process for desalination of heavy metal ions from an aqueous solution: kinetics and rate of recovery, *ACS ES&T Water*, 1 (2021) 134–144.
- [2] P. Sahu, Clathrate hydrate technology for water reclamation: present status and future prospects, *J. Water Process Eng.*, 41 (2021) 102058, doi: 10.1016/j.jwpe.2021.102058.
- [3] E.D. Sloan, C.A. Koh, *Clathrate Hydrates of Natural Gases*, CRC Press, Boca Raton, 2007. Available at: <https://www.crcpress.com/Clathrate-Hydrates-of-Natural-Gases/Jr-Koh-Koh/p/book/9780849390784>
- [4] J. Javanmardi, M. Moshfeghian, Energy consumption and economic evaluation of water desalination by hydrate phenomenon, *Appl. Therm. Eng.*, 23 (2003) 845–857.
- [5] S. Han, Y.-W. Rhee, S.-P. Kang, Investigation of salt removal using cyclopentane hydrate formation and washing treatment for seawater desalination, *Desalination*, 404 (2017) 132–137.
- [6] P. Sahu, S. Krishnaswamy, K. Ponnani, N.K. Pande, A thermodynamic approach to selection of suitable hydrate formers for seawater desalination, *Desalination*, 436 (2018) 144–151.
- [7] S. Ho-Van, B. Bouillot, J. Douzet, S. Maghsoodloo Babakhani, J.M. Herri, Cyclopentane hydrates – a candidate for desalination?, *J. Environ. Chem. Eng.*, 7 (2019) 103359, doi: 10.1016/J.JECE.2019.103359.
- [8] T. He, Z.R. Chong, P. Babu, P. Linga, Techno-economic evaluation of cyclopentane hydrate-based desalination with liquefied natural gas cold energy utilization, *Energy Technol.*, 8 (2020) 1900212, doi: 10.1002/ente.201900212.
- [9] D. Corak, T. Barth, S. Høiland, T. Skodvin, R. Larsen, T. Skjetne, Effect of subcooling and amount of hydrate former on formation of cyclopentane hydrates in brine, *Desalination*, 278 (2011) 268–274.

- [10] Y.-N. Lv, S.-S. Wang, C.-Y. Sun, J. Gong, G.-J. Chen, Desalination by forming hydrate from brine in cyclopentane dispersion system, *Desalination*, 413 (2017) 217–222.
- [11] J.-H. Cha, Y. Seol, Increasing gas hydrate formation temperature for desalination of high salinity produced water with secondary guests, *ACS Sustainable Chem. Eng.*, 1 (2013) 1218–1224.
- [12] F. Li, Z. Chen, H. Dong, C. Shi, B. Wang, L. Yang, Z. Ling, Promotion effect of graphite on cyclopentane hydrate based desalination, *Desalination*, 445 (2018) 197–203.
- [13] E.G. Dirdal, C. Arulanantham, H. Sefidroodi, M.A. Kelland, Can cyclopentane hydrate formation be used to rank the performance of kinetic hydrate inhibitors?, *Chem. Eng. Sci.*, 82 (2012) 177–184.
- [14] J. Zhang, P. Yedlapalli, J.W. Lee, Thermodynamic analysis of hydrate-based pre-combustion capture of CO₂, *Chem. Eng. Sci.*, 64 (2009) 4732–4736.
- [15] A.T. Trueba, L.J. Rovetto, L.J. Florusse, M.C. Kroon, C.J. Peters, Phase equilibrium measurements of structure II clathrate hydrates of hydrogen with various promoters, *Fluid Phase Equilib.*, 307 (2011) 6–10.
- [16] S. Han, J.-Y. Shin, Y.-W. Rhee, S.-P. Kang, Enhanced efficiency of salt removal from brine for cyclopentane hydrates by washing, centrifuging, and sweating, *Desalination*, 354 (2014) 17–22.
- [17] H. Xu, M.N. Khan, C.J. Peters, E.D. Sloan, C.A. Koh, Hydrate-based desalination using cyclopentane hydrates at atmospheric pressure, *J. Chem. Eng. Data*, 63 (2018) 1081–1087.
- [18] Z. Ling, C. Shi, F. Li, Y. Fu, J. Zhao, H. Dong, Y. Yang, H. Zhou, S. Wang, Y. Song, Desalination and Li⁺ enrichment via formation of cyclopentane hydrate, *Sep. Purif. Technol.*, 231 (2020) 115921, doi: 10.1016/j.seppur.2019.115921.
- [19] T. He, S.K. Nair, P. Babu, P. Linga, I.A. Karimi, A novel conceptual design of hydrate based desalination (HyDesal) process by utilizing LNG cold energy, *Appl. Energy*, 222 (2018) 13–24.
- [20] Z.R. Chong, T. He, P. Babu, J. Zheng, P. Linga, Economic evaluation of energy efficient hydrate based desalination utilizing cold energy from liquefied natural gas (LNG), *Desalination*, 463 (2019) 69–80.
- [21] B. Mottet, Method for Treating an Aqueous Solution Containing Dissolved Materials by Crystallization of Clathrate Hydrates, US20170044024A1, 2017.
- [22] M.H. Sharqawy, J.H. Lienhard, S.M. Zubair, The thermophysical properties of seawater: a review of existing correlations and data, *Desal. Water Treat.*, 16 (2010) 354–380.
- [23] R. Tanaka, Excess heat-capacities for mixtures of benzene with cyclopentane, methylcyclohexane, and cyclooctane at 298.15-K, *J. Chem. Eng. Data*, 30 (1985) 267–269.
- [24] H. Delroisse, F. Plantier, L. Marlin, C. Dicharry, L. Frouté, R. André, J.-P. Torré, Determination of thermophysical properties of cyclopentane hydrate using a stirred calorimetric cell, *J. Chem. Thermodyn.*, 125 (2018) 136–141.
- [25] A.S. Dalkilic, S. Wongwises, A performance comparison of vapour-compression refrigeration system using various alternative refrigerants, *Int. Commun. Heat Mass Transf.*, 37 (2010) 1340–1349.
- [26] I.S. Sandler, *Chemical, Biochemical, and Engineering Thermodynamics*, 5th ed., Wiley, Wiley India, New Delhi, 2006.
- [27] M.S. Peters, K.D. Timmerhaus, R.E. West, *Plant Design and Economics for Chemical Engineers*, 5th ed., McGraw-Hill Professional, New York, NY, 2002.
- [28] W.D. Seider, *Product and Process Design Principles: Synthesis, analysis, and Evaluation*, 2nd ed., Wiley, New York, 2004. Available at: <https://search.library.wisc.edu/catalog/999975575102121>
- [29] The Chemical Engineering Plant Cost Index, (n.d.). Available at: <https://www.chemengonline.com/pci-home> (accessed May 12, 2021).
- [30] J. Javanmardi, Kh. Nasrifar, S.H. Najibi, M. Moshfeghian, Economic evaluation of natural gas hydrate as an alternative for natural gas transportation, *Appl. Therm. Eng.*, 25 (2005) 1708–1723.
- [31] G.A. Al Bazedi, M.M. ElSayed, M. Amin, Comparison between reverse osmosis desalination cost estimation trends, *J. Sci. Eng. Res.*, 2016 (2016) 56–62.
- [32] P. Sahu, *Techno-Feasibility Studies on an Alternative Liquefied Natural Gas (LNG) Regasification Process Integrated with Freeze Desalination*, Birla Institute of Technology and Science, Pilani, India, 2019.
- [33] T. He, J. Zhang, N. Mao, P. Linga, Organic Rankine cycle integrated with hydrate-based desalination for a sustainable energy–water nexus system, *Appl. Energy*, 291 (2021) 116839, doi: 10.1016/j.apenergy.2021.116839.
- [34] H. Lee, H. Ryu, J.-H. Lim, J.-O. Kim, J. Dong Lee, S. Kim, An optimal design approach of gas hydrate and reverse osmosis hybrid system for seawater desalination, *Desal. Water Treat.*, 57 (2016) 9009–9017.